

## Quadratic transverse anisotropy term due to dislocations in $Mn_{12}$ acetate crystals directly observed by EPR spectroscopy

R. Amigó,<sup>1</sup> E. del Barco,<sup>1</sup> Ll. Casas,<sup>1,2</sup> E. Molins,<sup>1,2</sup> J. Tejada,<sup>1</sup> I. B. Rutel,<sup>3</sup> B. Mommouton,<sup>3,4</sup> N. Dalal,<sup>3</sup> and J. Brooks<sup>3</sup>

<sup>1</sup>*Departamento de Física Fundamental, Universidad de Barcelona, Diagonal 647, Barcelona, 08028, Spain*

<sup>2</sup>*Instituto de Ciencia de Materiales de Barcelona (CSIC), 08193 Cerdanyola, Spain*

<sup>3</sup>*NHMFL/FSU, CM/T group, 1800 E.P. Dirac Drive, Tallahassee, Florida 32310*

<sup>4</sup>*Institut National des Sciences Appliquées, Toulouse, France*

(Received 12 November 2001; published 9 April 2002)

High-sensitivity electron paramagnetic resonance experiments have been carried out in fresh and stressed  $Mn_{12}$  acetate single crystals for frequencies ranging from 40 GHz up to 110 GHz. The high number of crystal dislocations formed in the stressing process introduces a  $E(S_x^2 - S_y^2)$  transverse anisotropy term in the spin Hamiltonian. From the behavior of the resonant absorptions on the applied transverse magnetic field we have obtained an average value for  $E = 22$  mK, corresponding to a concentration of dislocations per unit cell of  $c = 10^{-3}$ .

DOI: 10.1103/PhysRevB.65.172403

PACS number(s): 75.45.+j, 75.50.Tt, 75.60.Lr

Since Friedman *et al.* found stepwise magnetic hysteresis on  $Mn_{12}$  acetate ( $Mn_{12}$ -Ac) molecular clusters and interpreted it in terms of resonant quantum tunneling,<sup>1</sup> a huge number of experimental measurements have been carried out on this compound<sup>2-10</sup> (see also references therein), showing its quantum behavior under many different experimental techniques, even at zero magnetic field. However, the uniaxial magnetic Hamiltonian of the  $Mn_{12}$  molecules cannot explain by itself the quantum behavior in the absence of external magnetic fields. Lowest-order transverse anisotropy terms and dipolar or hyperfine fields are not enough to explain the cited experimental data. Recently, Chudnovsky and Garanin<sup>11,12</sup> have suggested a theoretical approach which explains the quantum behavior of  $Mn_{12}$  Ac in terms of dislocations existing in the crystals. They propose that crystal dislocations introduce quadratic terms on  $S_x$  and  $S_y$ , producing tunneling in a lower order of perturbation theory than the transverse field. Unpublished experimental results seem to support this new theory.<sup>13-16</sup> In this paper we will show an experimental approach which indicates that dislocations formed in a strongly stressed single crystal introduce the  $E(S_x^2 - S_y^2)$  term suggested by Chudnovsky and Garanin, where  $E$  is the transverse anisotropy constant.

The  $Mn_{12}$ -Ac organometallic cluster forms a molecular crystal of tetragonal symmetry with lattice parameters  $a = 1.732$  nm and  $c = 1.239$  nm.<sup>17</sup> The unit cell contains two  $Mn_{12}O_{12}$  molecules surrounded by four water molecules and two acetic acid molecules. In the crystallization process point defects usually appear in a low number along the whole crystal. It has been shown experimentally that dislocations can be created in a  $Mn_{12}$ -Ac single crystal by rapid thermal cycles, in which a high change of temperature in a low scale of time produces radial and tangential tensions between the core and the surface of the crystal.<sup>14,15</sup> It is easy to visualize that tensions and pressure forces produced by mechanical distortion of the crystal may generate the same kind of dislocations in a single crystal. This is exactly what we have done with a  $Mn_{12}$ -Ac single crystal. When a dislocation is created inside the crystal it has produced a disorder of the molecules in the vicinity of the dislocation. As the number of dislocations in

the crystal grows the disorder extends over the whole crystal, converting it into a mosaic crystal. The mosaicity is related to the number of dislocations existing in the crystal and can be determined experimentally by analyzing the width of the x-ray diffraction peaks.<sup>18-20</sup>

In our experiments we have used two single crystals: (a) fresh single crystal and (b) strongly stressed single crystal. To distort the crystal we put it in a glue by one of the extremities. Then a gradually increasing force was applied to the other extreme, perpendicular to the longer length, until the crystal fractured. Then, the longer resulting part of the crystal was adequately cleaned and tested by x-ray diffraction to be sure that it was a single crystal. Both samples were characterized by x-ray analysis before making the EPR experiments. We used a four-circle single-crystal x-ray diffractometer (Enraf-Nonius CAD4, Mo  $K\alpha$  radiation) in the characterization. Reflections  $(\pm 2, \pm 2, \pm 2)$  were studied for both fresh and stressed single crystals. Peak intensities of the stressed crystal were normalized according to the measured volume of the studied fragment. Figure 1 shows a  $\Delta\omega - \Delta(2\theta)$  contour plot of  $(2, 2, -2)$  reflection for the fresh (left) and stressed crystal (right). An enlargement of the peak width along the  $\omega$  direction is clearly observed, although there is no significant change along the  $2\theta$  direction. Assuming that the distance between dislocations is inversely related to the widening of the reflection peak in the  $\omega$  direction<sup>14,18</sup> we can conclude that the number of dislocations increases about one order of magnitude in the distortion process.

The high-frequency resonance experiments have been carried out using the  $AB$  millimeter wave vector network analyzer (MVNA).<sup>21</sup> The base frequency obtained from this source (range 8–18 GHz) is multiplied by  $Q$ ,  $V$ , and  $W$  Schottky's diodes to obtain the frequency range used in our experiment (37–109 GHz). The sample—a single  $Mn_{12}$ -Ac crystal—is placed on the bottom of the cylindrical resonant cavity, halfway between its axis and perimeter. The applied dc magnetic field is parallel to the cavity axis and approximately perpendicular to the easy ( $c$ ) axis of the crystal. The experiment frequencies are  $TE_{0np}$  ( $n, p = 1, 2, 3, \dots$ ) which are the resonant frequencies for the cavity used. The reso-

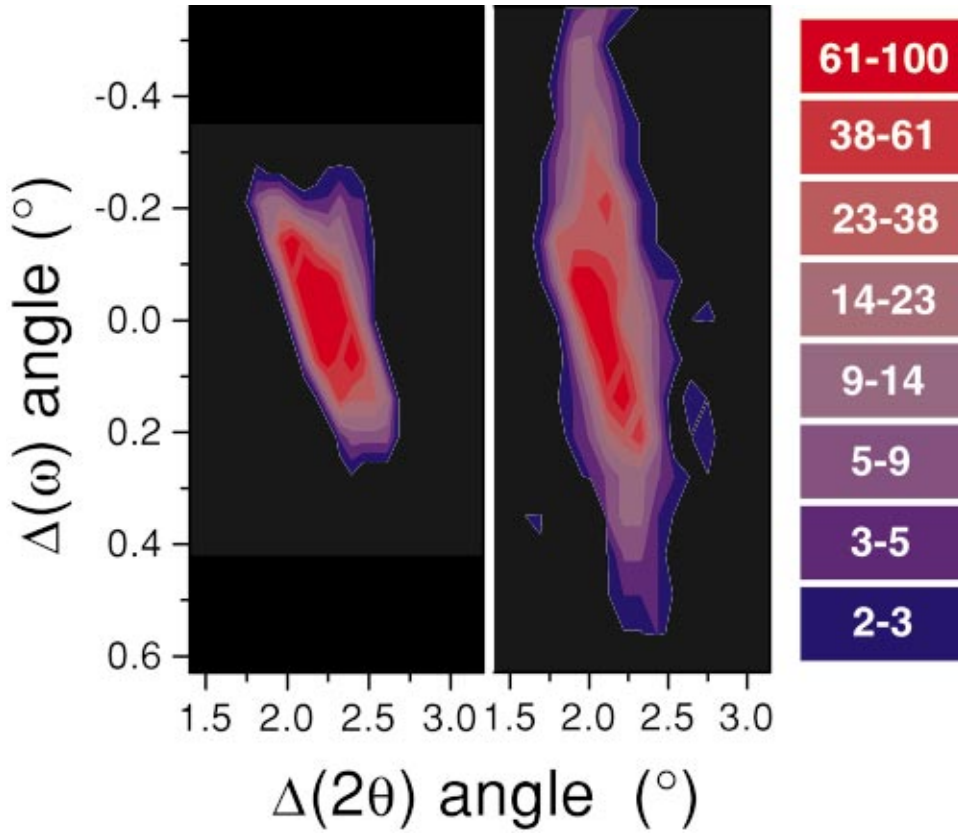


FIG. 1. (Color)  $\Delta\omega-\Delta(2\theta)$  contour plot of both fresh (left) and stressed (right)  $\text{Mn}_{12}\text{-Ac}$  single crystals for  $(2,2,-2)$  reflection. Increase of imperfections is evidenced by broadening along  $\omega$  direction.

nance  $Q$  factor varies from 20 000 at the  $\text{TE}_{011}$  mode (41.6 GHz) to a few thousand at higher frequencies.

The spin Hamiltonian used to explain the experimental data obtained in the last years is

$$\mathcal{H} = -DS_z^2 - BS_z^4 + C(S_+^4 + S_-^4) - g\mu_B \mathbf{H} \cdot \mathbf{S}, \quad (1)$$

where  $D$ ,  $B$ , and  $C$  have been experimentally obtained by electron paramagnetic resonance (EPR), neutron spectroscopy, and magnetic relaxation experiments.<sup>1-6,9,10,22</sup>  $\mathbf{H}$  is the applied magnetic field. In the absence of longitudinal field, the quantum splitting of the different  $m$  spin levels,  $\Delta_m$ , and consequently the rate of resonant tunneling between the spin levels depend on the magnitude of the transverse component  $H_\perp$ . In the transmission spectra of our EPR experiments we can detect absorptions peaks corresponding to the absorption of radiation of frequency  $f$  by the transitions effectuated between the spin levels of the Hamiltonian with energy difference equal to  $hf$ . From the field position of these peaks we can extract the behavior of the quantum splittings on the transverse magnetic field. The results obtained with the fresh crystal are plotted in Fig. 2 (solid circles). We have found the best fitting of our data for  $D=555$  mK,  $B=1.3$  mK, and  $C=2.2 \times 10^{-2}$  mK (solid lines in Fig. 2), in good agreement with the values given in Refs. 6 and 22. From this figure, it is clearly observed that the dependence of the quantum splittings ( $\Delta_{10}$  first right line,  $\Delta_9$  second,  $\Delta_8$  third, and so on) on the transverse field matches perfectly with the theoretical calculation. The lines that appear at high frequencies and round going down and up with the field correspond to the energy difference between different quantum splittings.

In Fig. 3 we show the EPR absorption spectra recorded at

$f = 67$  GHz for both fresh (A) and stressed (B)  $\text{Mn}_{12}\text{-Ac}$  single crystals. The labeling used in the figure  $\alpha_{m,\varphi}$  refers to the  $\Delta_m$  splitting absorptions with the field applied perpendicular to the easy axis with an angle,  $\varphi$ , with respect to the  $x$  magnetic axis. For a fresh crystal, represented by the Hamiltonian (1), there is a symmetry between any direction perpendicular to the easy axis. The peaks observed for fresh

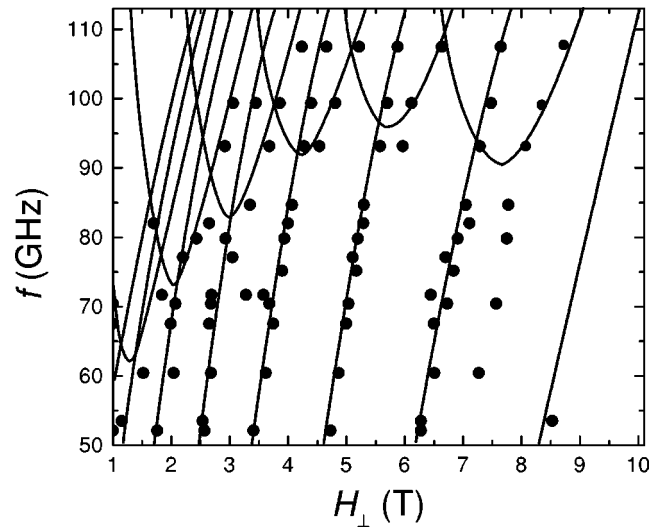


FIG. 2. Resonant peaks from fresh single crystal of  $\text{Mn}_{12}\text{-Ac}$  for different frequencies, ranging from 50 GHz up to 110 GHz, as a function of the magnetic field applied perpendicularly to the magnetic easy axis direction of the crystal. The solid lines are the fitting result of the diagonalization of the spin Hamiltonian of Eq. (1).

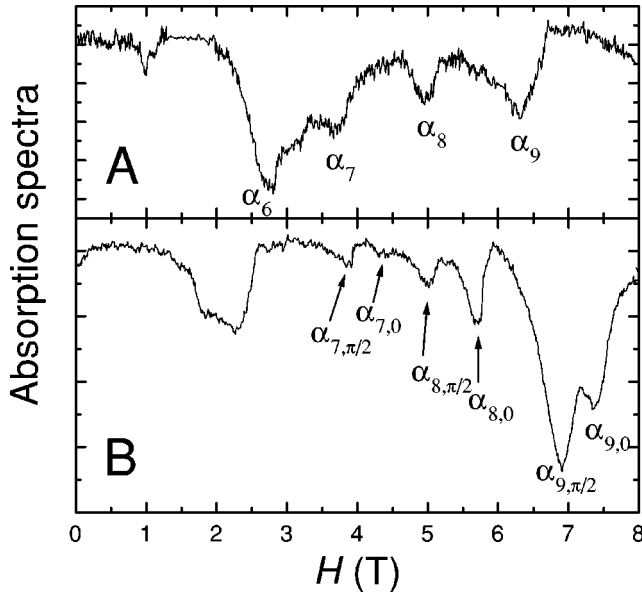


FIG. 3. EPR spectra recorded at 67 GHz for both fresh (A) and stressed (B) single crystals of  $\text{Mn}_{12}\text{-Ac}$ . The experiments were done at  $T=10$  K. The peaks are associated to the different quantum splittings through the next nomenclature:  $\Delta_{m,\varphi}$ .

crystal correspond to the resonances with the splittings  $\Delta_9$ ,  $\Delta_8$ ,  $\Delta_7$ , and so on, as is shown in Fig. 2. However, for the stressed crystal, each  $\alpha_m$  absorption peak appears doubled. This phenomenon can be explained by the addition of a  $E(S_x^2 - S_y^2)$  term to the Hamiltonian (1). This term introduces the hardest anisotropy along the  $x$  axis, while the  $y$  axis remains as a medium anisotropy axis. For this reason, different directions of the applied field give different values of each quantum splitting,  $\Delta_{m,\varphi}$ . This is the same behavior observed in the powder sample of  $\text{Fe}_8$  molecular clusters.<sup>23,24</sup> The angular dependence of  $\Delta(\varphi)$  at a fixed value of the transverse component of the field is not monotonic. Because of the shape of the function  $\Delta(\varphi)$ , for a sample with hard axis oriented at random—that is, with no preference for any angle  $\varphi$ —there are two values of  $\Delta$  for which the density of states has a peak. These are the values of the splitting corresponding to  $\varphi=0$  and  $\varphi=\pi/2$  (see Refs. 23 and 24). In the absence of dissipation, the contribution of each  $\text{Mn}_{12}$  molecule to the imaginary part of the susceptibility is proportional to  $\delta(\omega - \Delta[\varphi, H_\perp]/\hbar)$ . However, the total imaginary part of the susceptibility is

$$\chi'' \propto \int_0^\pi g(\varphi) \delta\left(\omega - \frac{\Delta[\varphi, H_\perp]}{\hbar}\right) d\varphi, \quad (2)$$

where  $g(\varphi)$  is the distribution of molecules on  $\varphi$ . For a fresh crystal, having no significant number of dislocations, there is an equivalence between the  $x$  and  $y$  axes as the Hamiltonian (1) has no preference for any transverse direction. Due to this, the splitting does not depend on  $\phi$  and the amplitude  $A$  of the absorption of electromagnetic radiation must have only one peak corresponding to  $\Delta[H_\perp]=hf$ , as can be seen in Figs. 2 and 3(A). On the contrary, in a strongly stressed single crystal of  $\text{Mn}_{12}$  the dislocations are randomly affecting the magnetic structure of the molecular clusters, introducing

the term  $E(S_x^2 - S_y^2)$  in a different manner for each molecule.<sup>11,12</sup> For this reason, a  $\text{Mn}_{12}\text{-Ac}$  single crystal with a large mosaicity can be approximated as a powder sample with the  $x$  axis of the molecules oriented at random. In this case, Eq. (2) can be rewritten as

$$\chi'' \propto \int_0^\infty \delta\left(\omega - \frac{\Delta[\varphi, H_\perp]}{\hbar}\right) \left(\frac{d\Delta}{d\varphi}\right)^{-1} d\Delta = \left(\frac{d\Delta}{d\varphi}\right)^{-1} \Big|_{\Delta=\hbar\omega}. \quad (3)$$

Therefore, there are two field values, solutions of the equations  $\Delta[0, H_{\perp 1}] = hf$  and  $\Delta[\pi/2, H_{\perp 2}] = hf$ , at which the amplitude of the absorption is maximal. Due to this, the two doubled peaks of each splitting observed in the stressed single crystal [Fig. 3(B)] can be attributed to the two mean orientations of the splitting  $\Delta$  on the angle  $\varphi$ :  $\Delta_{m,0}$  and  $\Delta_{m,\pi/2}$ . As the distance between the two doubled peaks basically depends on the parameter  $E$  we can extract a first value,  $E \sim 20$  mK.

A more precise analysis of the effect of dislocations on the spin Hamiltonian of  $\text{Mn}_{12}\text{-Ac}$  can be achieved by studying the behavior of the quantum splittings on the transverse magnetic field. In Fig. 4, it has been plotted the field position of the EPR absorption peaks found at the experiment frequencies  $f$  for the stressed crystal (open circles). The EPR data have been fitted by using the magnetic level structure resulting from diagonalization of the Hamiltonian (1), adding the term  $E(S_x^2 - S_y^2)$  attributed to the effect of the dislocations. The results of our fitting procedure are shown in Fig. 4. Black lines correspond to  $\varphi=0$  and blue lines correspond to  $\varphi=\pi/2$ . The values of the Hamiltonian parameters used in our fitting procedure are  $D=675$  mK,  $B=0.9$  mK,  $C=1.8 \times 10^{-2}$  mK, and  $E=22$  mK. Comparing these values with the values extracted from the fitting of the fresh crystal absorption peaks of Fig. 2 one can conclude that dislocations introduce a general variation of the spin Hamiltonian. This effect of dislocations on the magnetic structure of the molecules on the vicinity is expected in the theoretical model of Chudnovsky and Garanin.<sup>11,12</sup> As the authors observe, dislocations may introduce other effects—for example, transverse magnetic fields. This effect has not been considered in our analysis because its complexity. However, we can extract quantitative information of the number of dislocations existing in the stressed single crystal by analyzing the distribution of the generated transverse anisotropies. From the theoretical model,<sup>12</sup> one can extract the distribution of the logarithm of the transverse anisotropy,  $\ln(E/2D)$ , as a function of the concentration of dislocations per unit cell,  $c$ . This distribution function has a maximum at a different value of  $E/2D$  depending on  $c$ . If we assume that the observed absorption peaks correspond to this maximum in the distribution, we can extract an approximated value of  $c$  from the Hamiltonian parameters resulting from the fitting procedure. We have obtained  $\ln(E/2D) = -4.1$ . This corresponds to a concentration of dislocations per unit cell of  $c \sim 10^{-3}$ , in good agreement with the theoretical estimation,<sup>12</sup> and with the experimental results<sup>13–15</sup> for similar samples. Using the comparison x-ray analysis of the mosaicity for both the fresh and stressed crystals of Fig. 1, one can observe that the number of dislocations is increased by almost one order of magnitude than the

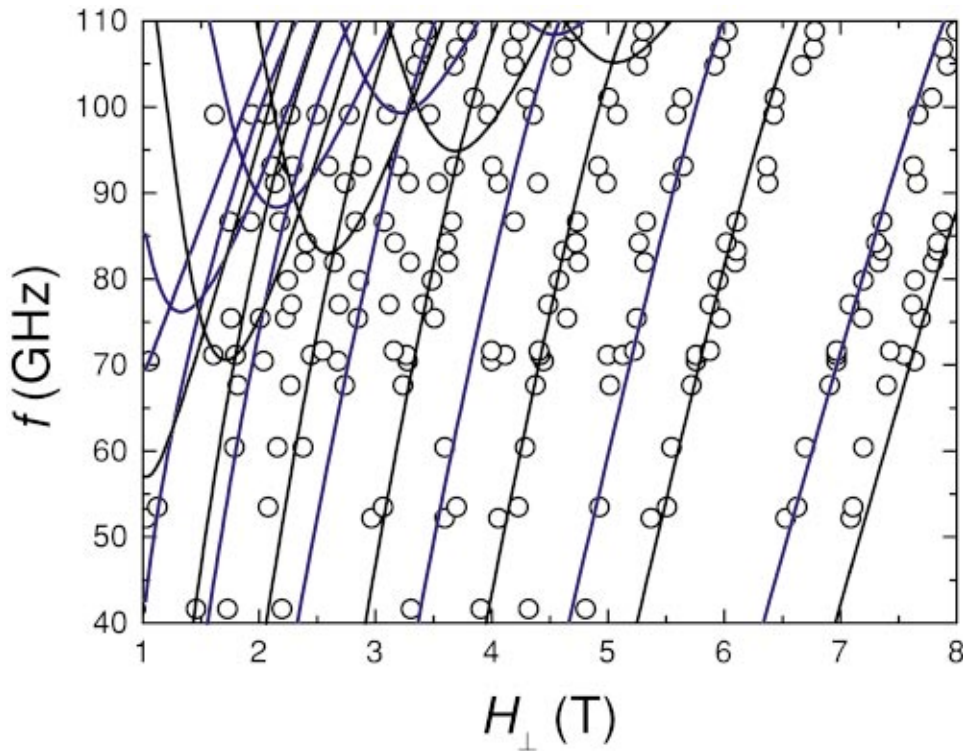


FIG. 4. (Color) EPR peaks for the stressed single crystal of  $\text{Mn}_{12}\text{-Ac}$ . The data are fitted by adding the term  $E(S_x^2 - S_y^2)$  to the Hamiltonian of Eq. (1). The fitting lines represent the field behavior of the quantum splittings for  $\varphi = 0$  (black lines) and  $\varphi = \pi/2$  (blue lines).

fresh sample. We conclude that in a fresh crystal the number of dislocations per unit cell is approximately  $c \sim 10^{-4}$ .

Through high-sensitivity EPR experiments carried out in a strongly stressed single crystal of  $\text{Mn}_{12}$  acetate we have directly obtained the magnitude of the transverse anisotropy term  $E(S_x^2 - S_y^2)$ , with  $E = 22$  mK, associated with dislocations existing in the crystal. It may be also possible that the combined effect of a heavy x-ray irradiation dose and subsequent thermal stressing treatment creates a large number of new defective sites and extends the original ones. These sites will necessarily have a lower symmetry and could lead to new EPR absorption peaks, with an  $E$  term,

such as determined here. A clear effect of lattice defects on magnetization tunneling has been detected recently.<sup>13–15</sup> We also note that an EPR line-broadening effect of naturally present defects in  $\text{Mn}_{12}$  and  $\text{Fe}_8$  single crystals has been reported recently.<sup>25</sup> Additional investigations are thus needed in order to clearly understand the origin of the newly found EPR peaks in the present work.

This work was supported by MEC Grant No. PB-96-0169 and EC Grant No. IST-1929. Work at NHMFL/FSU was supported through a contractual agreement between the NSF through Grant No. NSF-DMR-95-27035 and the State of Florida.

<sup>1</sup>J. R. Friedman *et al.*, Phys. Rev. Lett. **76**, 3830 (1996).

<sup>2</sup>J. M. Hernandez *et al.*, Europhys. Lett. **35**, 301 (1996).

<sup>3</sup>L. Thomas *et al.*, Nature (London) **383**, 145 (1996).

<sup>4</sup>F. Luis *et al.*, Nanotechnology **10**, 86 (1999).

<sup>5</sup>J. A. A. Perenboom *et al.*, Phys. Rev. B **58**, 330 (1998).

<sup>6</sup>S. Hill *et al.*, Phys. Rev. Lett. **80**, 2453 (1998).

<sup>7</sup>A. Fort *et al.*, Phys. Rev. Lett. **80**, 612 (1998).

<sup>8</sup>W. Wernsdorfer, R. Sessoli, and D. Gatteschi, Europhys. Lett. **47**, 254 (1999).

<sup>9</sup>L. Bokacheva, A. D. Kent, and M. A. Walters, Phys. Rev. Lett. **85**, 4803 (2000).

<sup>10</sup>A. D. Kent *et al.*, Europhys. Lett. **49**, 521 (2000).

<sup>11</sup>E. M. Chudnovsky and D. A. Garanin, Phys. Rev. Lett. **87**, 187203 (2001).

<sup>12</sup>D. A. Garanin and E. M. Chudnovsky, Phys. Rev. B **65**, 094423 (2002).

<sup>13</sup>K. M. Mertens *et al.*, Phys. Rev. Lett. **87**, 227205 (2001).

<sup>14</sup>J. M. Hernandez *et al.*, cond-mat/0110515 (unpublished).

<sup>15</sup>F. Torres *et al.*, cond-mat/0110538 (unpublished).

<sup>16</sup>The combination of both x-ray irradiation and mechanical stressing may be additive in the process of dislocations and defects creation.

<sup>17</sup>T. Lis, Acta Crystallogr., Sect. B: Struct. Crystallogr. Cryst. Chem. **36**, 4024 (1980).

<sup>18</sup>R. I. Barabash, in *Defect and Microstructure Analysis by Diffraction*, edited by R. L. Snyder, J. Fiala, and H. J. Bunge, IUCr Monographs on Crystallography 10 (Oxford University Press, Oxford, 1999), pp. 127–140.

<sup>19</sup>A. McL. Mathieson, Acta Crystallogr., Sect. A: Cryst. Phys., Diffraction, Theor. Gen. Crystallogr. **38**, 378 (1982).

<sup>20</sup>A. McL. Mathieson and A. W. Stevenson, Acta Crystallogr., Sect. A: Found. Crystallogr. **41**, 223 (1986).

<sup>21</sup>Manufactured by Abmm, 52 Rue Lhomond, 75005 Paris, France.

<sup>22</sup>A. L. Barra, D. Gatteschi, and R. Sessoli, Phys. Rev. B **56**, 8192 (1997).

<sup>23</sup>E. del Barco *et al.*, Europhys. Lett. **47**, 722 (1999).

<sup>24</sup>E. del Barco *et al.*, Phys. Rev. B **62**, 3018 (2000).

<sup>25</sup>K. Park, M. Novotny, N. S. Dalal, S. Hill, and P. Rikvold, Phys. Rev. B **65**, 014426 (2002).